Theoretical Studies of Nuclear Magnetic Resonance Parameters for the Proton-Exchange Pathways in Porphyrin and Porphycene

Hubert Cybulski

Department of Chemistry, University of Tromsø, N-9037 Tromsø, Norway, Department of Chemistry, University of Oslo, Box 1033 Blindern, N-0315 Oslo, Norway, and Department of Chemistry, University of Warsaw, Pasteura 1, 02-093 Warszawa, Poland

Magdalena Pecul*

Department of Chemistry, University of Warsaw, Pasteura 1, 02-093 Warszawa, Poland, and Department of Chemistry, University of Tromsø, N-9037 Tromsø, Norway

Trygve Helgaker

Department of Chemistry, University of Oslo, Box 1033 Blindern, N-0315 Oslo, Norway

Michał Jaszuński

Institute of Organic Chemistry, Polish Academy of Sciences, Kasprzaka 44, 01-224 Warszawa, Poland

Received: October 6, 2004; In Final Form: January 12, 2005

The nuclear magnetic resonance (NMR) parameters in porphyrin and porphycene have been calculated to investigate their changes during the process of proton exchange, using density-functional theory (DFT) for both the spin−spin coupling constants and the shielding constants. In addition, in calculations on the smaller 1,3-bis(arylimino)isoindoline molecule, we have tested the performance of our computational approach against experimental data. The calculated nuclear spin−spin coupling constants and shielding constants have been analyzed as functions of the progress of the proton transfer between two nitrogen atoms. The one-bond couplings between proton and nitrogen, dominated by the Fermi-contact term, decay steeply as the internuclear distance increases. The small changes in the intramolecular J_{HH} coupling between two inner protons are mainly determined by the sum of relatively large spin−orbit terms. The isotropic shielding constant shows a strong deshielding of the nitrogen nuclei as the proton migrates away. Both the isotropic shielding of the exchanged protons and the shielding anisotropy exhibit a minimum close to the transition states.

I. Introduction

Nuclear magnetic resonance (NMR) spectroscopy is a powerful tool for the investigation of molecular structure, in particular, for the study of hydrogen bonding.[1−9] NMR shielding constants (or chemical shifts) have for a long time been used as sensitive probes of molecular environment, and the ^{1}H NMR shielding constant is a well-established parameter of hydrogen-bond strength[1] and an indicator of proton transfer; ^{15}N shielding constants are also frequently used for this purpose.[3,10,11] Recently, NMR techniques have been refined to the extent that spin−spin coupling constants can be used as parameters of hydrogen bonds.[12−17] The small hydrogen-bond-transmitted coupling constants are particularly promising in this respect.[13−17] The development of experimental NMR is accompanied by advances in theoretical methods and computational power, allowing the ab initio wave function or density-functional calculation of NMR shielding constants and spin−spin coupling constants (much more demanding computationally) in large systems of chemical interest.[18−21] This progress in computational techniques has made possible the use of ab initio methods for the interpretation and prediction of experimental NMR spectra for fairly large systems, such as those investigated in the present work.

In this work, we study the free-base porphyrin and the structurally related porphycene molecule. Porphyrin and related compounds are found in nearly all living organisms, playing a fundamental role in many biological processes such as oxygen absorption and transport (hemoglobin), oxygen activation (cytochrome *c*), and the initial photochemical step in photosynthesis (chlorophyll). Porphyrins are among the best ligands in terms of thermodynamic stability and kinetic nonlability, having the perfect size to bind nearly all metal ions. Because of their unique physical, chemical, and biological properties, porphyrin and porphyrin-like molecules are among the most widely studied macrocyclic systems.

The proton tautomerism of heterocyclic compounds, in particular, of the porphyrins, is a topic of continuing interest because of its intimate relation to many molecular properties and, consequently, to processes such as photosynthesis and metal-coordination reactions. The general interest in free-base porphyrins and in the mechanism of proton transfer has also been raised by the dispute about the role of short, strong hydrogen bonds in enzymatic catalysis.[22−26] Several experi-

* Corresponding author. E-mail: mpecul@chem.uw.edu.pl.

10.1021/jp045440h CCC: $30.25
Published on Web 04/16/2005

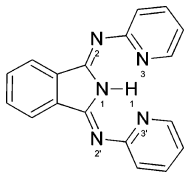

Figure 1. Structure of 1,3-bis(arylimino)isoindoline (2ABAI).

mental studies have used NMR to investigate proton transfer in free-base porphyrin[27] and free-base porphycene.[28] However, apart from some calculations of shieldings on one free-base porphyrin structure,[29,30] our study is the first that uses electronic-structure theory to examine the changes in the spin−spin and shielding constants induced by intramolecular proton transfer in free-base porphyrin and porphycene. For biological systems that are active in aqueous environments, one should also consider the interplay of intramolecular proton transfer and intermolecular proton exchange, but this is less important for free-base molecules and we restrict ourselves here to intramolecular processes.

We are not aware of any experimental measurements of the spin−spin coupling constants of central nitrogen atoms and free-base protons in porphyrin or porphycene, but some experimental results are available for the shielding constants.[27−32] Measurements of the spin−spin couplings of interest are difficult because of the fast proton exchange (especially in porphycene), requiring drastically lowered temperatures to separate the signals. Since a comparison with experiment helps to ascertain the reliability of the calculations, we have here also analyzed the NMR spectrum of a smaller molecule where a proton may be migrating between nitrogen atoms of the aromatic rings, namely, 1,3-bis-(arylimino)isoindoline (see Figure 1). For this molecule, experimental NMR spectra, including many spin−spin coupling constants, have been collected by Schilf.[33]

The structure of this paper is as follows: First, we describe the computational methods used in this study. In the next section, the results of the calculations are discussed, beginning with the spin−spin coupling constants and NMR shielding constants of porphyrin, porphycene, and 1,3-bis(arylimino)isoindoline in their global minimum form and proceeding to the effects of the single and double proton transfers in porphyrin and porphycene. Finally, we give a brief summary and some concluding remarks.

II. Computational Details

The structures of porphyrin, porphycene, and 1,3-bis(arylimino)isoindoline (2ABAI in the notation of ref 33) were optimized by means of density-functional theory (DFT), using the Becke−three-parameter−Lee−Yang−Parr (B3LYP) hybrid functional[34] as implemented in the Gaussian 98 program.[35] In these calculations, we used the 6-31G** basis set. In the studies of the proton transfer, the geometry was reoptimized with the distances between the migrating protons and associated nitrogen atoms kept fixed at a given value.

The calculations of the indirect nuclear spin−spin coupling constants and the NMR shielding constants were carried out using DFT with the B3LYP functional,[34] as implemented in a development version of the DALTON program;[36] see ref 37 for the implementation of spin−spin constants and ref 38 for the implementation of shielding constants. For the evaluation of shielding constants, London orbitals were used to ensure gauge-origin independence.[39]

The 6-31G** basis set, which was used for the geometry optimizations, is not suitable for the calculation of NMR properties. Still, since porphyrins are relatively large molecules, our choice of basis set represents a compromise between the desired accuracy and the available computational resources. Fortunately, since NMR shielding and spin−spin coupling constants are local properties, it is possible to use locally dense basis sets, which describe accurately only the region of a molecule that is important for a given set of parameters. We therefore used a basis consisting of Huz-IIsu2 functions (obtained from the Huz-II basis set[40] by decontracting the *s* functions and adding two tight *s* functions[41]) on the nitrogens and migrating protons of porphyrin and porphycene and 6-31G** functions on the remaining atoms. Test calculations with Huz-IIsu2 functions on all atoms confirmed that this basis set is sufficiently flexible for our purposes; the NMR properties of the nitrogens and inner protons calculated with the locally dense and full basis sets are reasonably close to each other. The NMR calculations on the smaller 2ABAI molecule were carried out in the full Huz-IIsu2 basis.

III. Results and Discussion

A. Molecular Geometries. *1. 1,3-Bis(arylimino)isoindoline Molecule.* The optimized 1,3-bis(arylimino)isoindoline structure is planar; see Figure 1. The calculated bond lengths agree reasonably well with the X-ray data in ref 33, with the only exception being the optimized N1−H1 distance 1.0173 Å, which is significantly longer than the experimental value 0.92(2) Å. Since the X-ray data were obtained for the solid state, this disrepancy may in part arise from intermolecular interactions and from experimental errors (note the large error bar).

2. Porphyrin and Porphycene Molecules. In the course of the geometry optimization, we found two planar energy minima of porphyrin (trans and cis, see Figure 2) and two planar minima of porphycene (trans and cis1, see Figure 3). The agreement between the optimized and crystallographic structures is satisfactory for both porphyrin[42] and porphycene.[32] As for 2ABAI, the largest difference is observed for the nitrogen−inner-proton distance.

The trans structure of porphyrin (the global minimum) lies 34.3 kJ/mol below the cis structure, which is a local minimum. For porphycene, the energy difference between the local cis1 minimum and the global trans minimum is only 9.3 kJ/mol, while the cis2 structure is a saddle point, 138.4 kJ/mol higher than the global minimum. These results agree with previous findings on the tautomers of porphyrin and porphycene.[43−45]

Several processes involve the transfer of a single proton from the trans to cis structures. In each case (i.e., for the trans-to-cis pathway in porphyrin and for the trans-to-cis1 and trans-to-cis2 pathways in porphycene), we localized the transition state. In addition, two pathways involving the simultaneous transfer of two protons were examined—specifically, the path connecting two equivalent trans structures and that connecting two equivalent cis (cis1) structures. In both molecules, the trans-to-trans′ and cis-to-cis′ (cis1-to-cis1′) pathways intersect at a second-order saddle point (SS in Figures 2 and 3), with two imaginary vibrational frequencies corresponding to trans-to-trans′ and cis-to-cis′ (cis1-to-cis1′) transitions, respectively.

The trans-to-trans′ interconversion can also occur as a two-step concerted asynchronous mechanism, via the cis structure, with only one proton migrating in each step, in agreement with the potential energy surface of porphyrin discussed by Baker et al.[46] Similarly, the cis-to-cis′ (cis1-to-cis1′) tautomeric change can occur as a two-step concerted asynchronous mechanism, via the trans structure. In porphycene, there is also the possibility of the trans-to-trans′ proton transfer via the cis2 structure. However, since cis2 is a saddle point of high energy, this

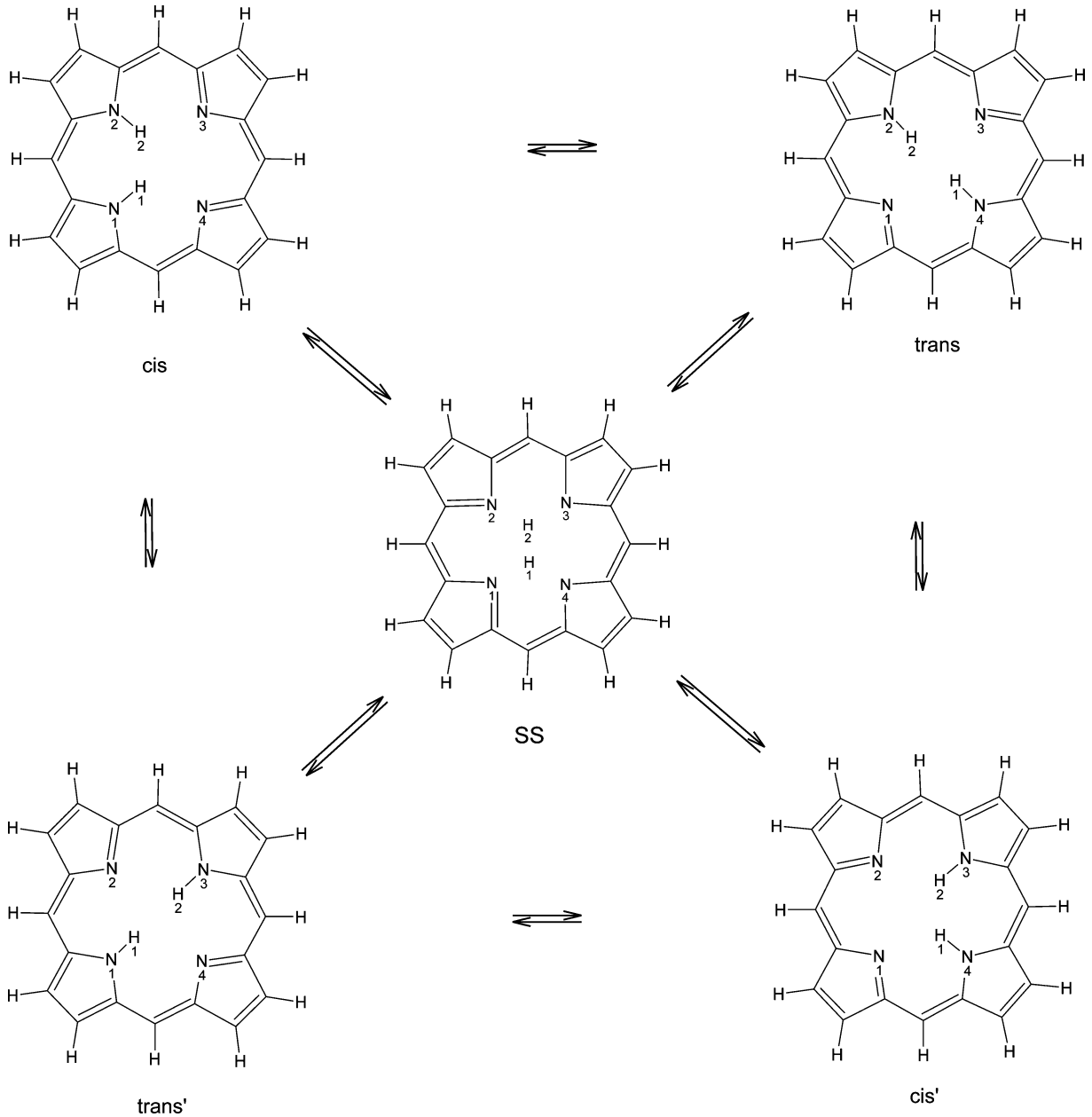

Figure 2. Proton-exchange pathways for the porphyrin molecule. The global energy minimum corresponds to the trans structure, and the second-order saddle point (SS) in the middle is common for the trans-to-trans′ and cis-to-cis′ pathways.

pathway is energetically unfavorable (albeit accessible at room temperature).

In Figure 4, we have, for each proton-transfer pathway, plotted the energy as a function of the distance from the migrating proton to the originating nitrogen atom. In porphyrin, the trans-to-cis barrier is 63.9 kJ/mol (forward) and 29.7 kJ/mol (backward); in porphycene, the corresponding trans-to-cis1 barrier is much smaller: 17.2 kJ/mol (forward) and 7.8 kJ/mol (backward).

Since the trans-to-trans′ and cis-to-cis′ (cis1-to-cis1′) pathways pass through the same saddle point, their relative barrier heights depend only on the energies of the trans and cis (cis1) structures. In porphyrin, the trans-to-trans′ barrier of 94.2 kJ/mol is higher than the trans-to-cis barrier of 63.9 kJ/mol, while the cis-to-cis′ barrier of 60.0 kJ/mol is higher than the cis-to-trans barrier of 29.7 kJ/mol. Likewise, in porphycene, the trans-to-trans′ barrier of 25.6 kJ/mol is higher than the trans-to-cis1 barrier of 17.2 kJ/mol, while the cis1-to-cis1′ barrier of 16.3 kJ/mol is higher than the cis1-to-trans′ barrier of 7.8 kJ/mol. The fourth proton-exchange pathway in porphycene, trans-to-cis2 (part of the high-energy trans-to-trans′ pathway), exhibits the highest barrier for the proton to overcome: 183.4 kJ/mol (forward) and 45.0 kJ/mol (backward). The experimental values of the effective proton-transfer barrier from ^{15}N solid-state NMR data are 51.4 and 31.8 kJ/mol, respectively, for porphyrin and porphycene.[28] Our results for porphyrin therefore appear to be too high, whereas the values for porphycene are somewhat too low. Finally, we note that, in a more detailed analysis of the relative energy differences discussed here, one should also take into account molecular vibrations.

B. NMR Parameters for 1,3-Bis(arylimino)isoindoline. The spin−spin coupling constants and NMR shielding constants for 2ABAI are collected in Table 1, where comparisons are made with experimental data.[33] The shielding constants of the inner-ring nitrogen nuclei differ considerably from each other. Whereas the nitrogen nucleus N1 bound to the hydrogen nucleus H1 is shielded (positive shielding constant), the N2 and N3 nuclei are deshielded. These results are in good agreement with

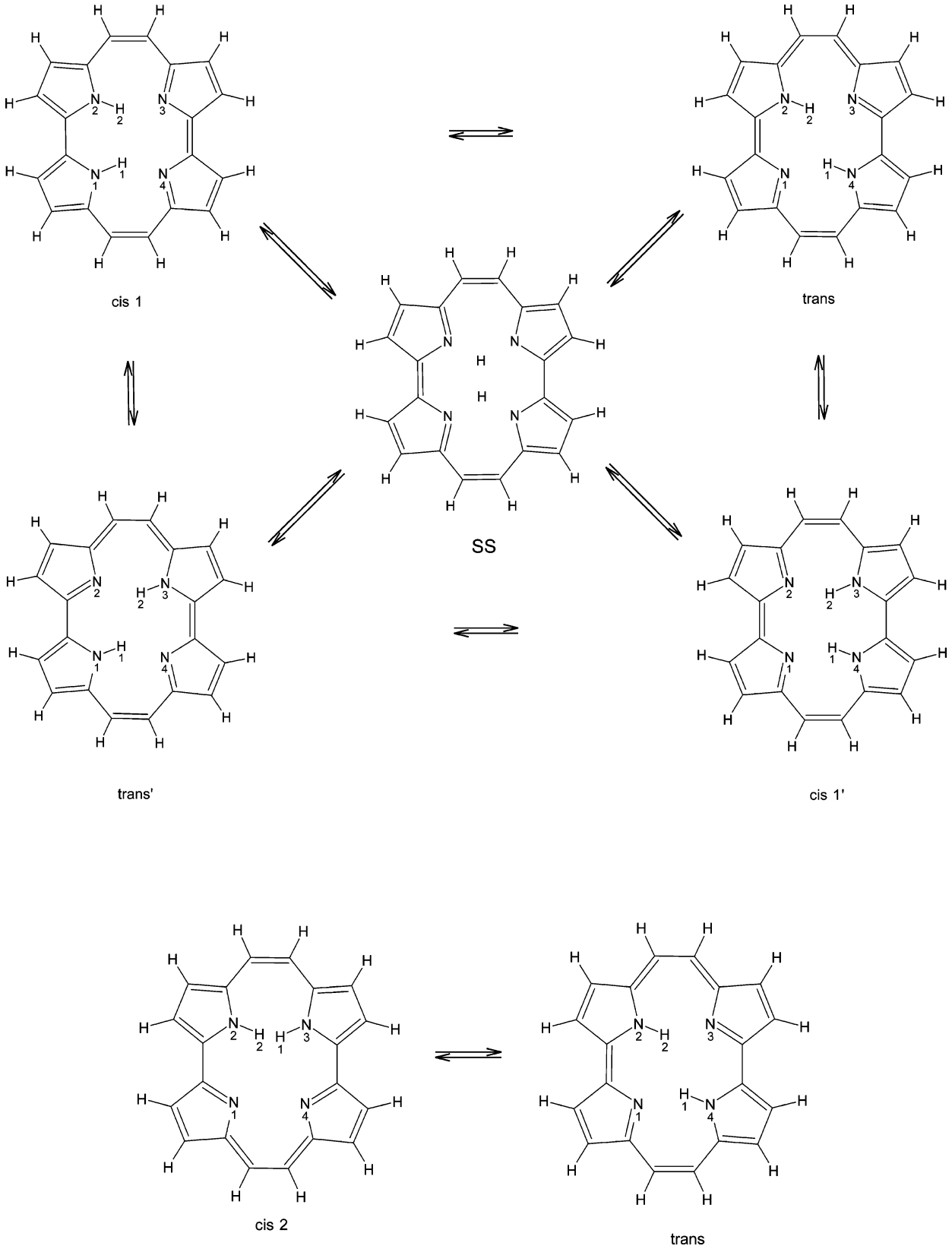

Figure 3. Proton-exchange pathways for the porphycene molecule. The global energy minimum corresponds to the trans structure, and the second-order saddle point (SS) in the middle is common for the trans-to-trans′ and cis-to-cis′ pathways.

experiment—when shifted by −135.0 ppm (the reference is liquid nitromethane), the experimental values differ systematically by only about 20 ppm from the theoretical values. In part, this difference can be attributed to an uncertainty in the shielding constant of the reference. The calculated coupling constant $^1J_{N1H1}$ of −109.23 Hz is also in good agreement with the experimental value 98.5 Hz (the sign is not determined in experiment, and we discuss the coupling constants for ^{15}N). The relatively large value (2.43 Hz) of the J_{N3H1} coupling, transmitted through the internal hydrogen bond in 2ABAI, indicates that

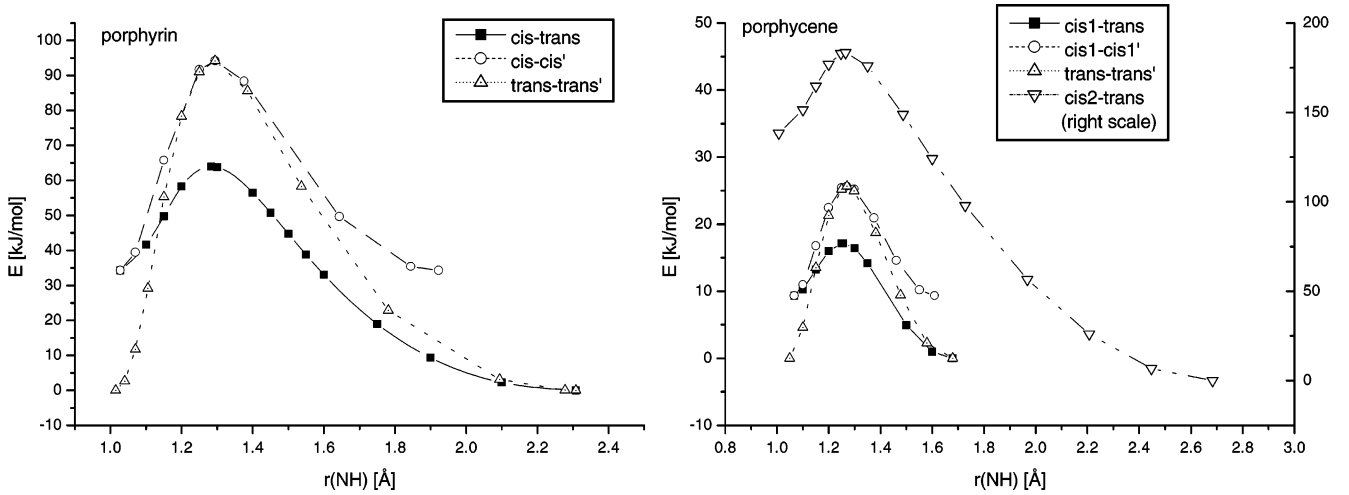

Figure 4. Dependence of the energy of porphyrin (left, in kJ/mol) and porphycene (right, in kJ/mol) on the distance between the migrating proton and parent nitrogen atom (in Å). For the cis2-to-trans pathway in porphycene, the scale is given on the right.

TABLE 1: Spin−Spin Coupling Constants (Hz) and Shielding Constants (ppm) for the 1,3-Bis(arylimino)isoindoline Molecule

	value	
parameter	calcd	exptl[a]
J_{N1H1}	−109.23	98.5[b]
J_{N2H1}	−0.08	
J_{N3H1}	2.43	
σ^{iso}_{H1}	18.59	
σ^{aniso}_{H1}	−22.15	
σ^{iso}_{N1}	84.47 (−219.5[c])	−239.0
σ^{aniso}_{N1}	132.45	
σ^{iso}_{N2}	−11.52 (−123.5[c])	−146.2
σ^{iso}_{N3}	−70.46 (−64.5[c])	−88.4
σ^{aniso}_{N3}	498.95	

[a] Experimental values taken from ref 33. [b] Sign not measured. [c] For comparison with experiment, chemical shifts obtained assuming −135.0 ppm as the shielding of the reference (nitromethane).

TABLE 2: Spin−Spin Coupling Constants (Hz), Shielding Constants (ppm), and Chemical Shifts for the Global Energy Minima (trans Structures) of Porphyrin and Porphycene

parameter	porphyrin	porphycene
J_{H1H2}	1.38	1.18
J_{N1H1}	1.70	3.28
J_{N2H1}	−0.12	−0.06
J_{N3H1}	1.70	0.15
J_{N4H1}	−108.47	−97.52

	calcd	exptl	calcd	exptl
σ^{iso}_{H1}	38.06 (−7.23[a])	−3.91[b]	31.10 (−0.27[a])	3.15[c]
σ^{aniso}_{H1}	32.90		23.89	
σ^{iso}_{N1}, σ^{iso}_{N3}	−11.36 (228.36[a])	215[d]	0.94	
σ^{aniso}_{N1}, σ^{aniso}_{N3}	424.87		361.80	
σ^{iso}_{N2}, σ^{iso}_{N4}	100.30 (116.70[a])	107[d]	83.95	
σ^{aniso}_{N2}, σ^{aniso}_{N4}	182.39		187.62	

[a] For comparison with experiment, chemical shifts obtained assuming 30.83 ppm as the shielding of the reference (TMS) for ^{1}H and 217 ppm as the shielding of the reference (NH_4Cl) for ^{15}N. [b] Experimental values taken from ref 29. [c] Experimental values taken from ref 32. [d] Experimental values taken from ref 31.

this coupling may be measurable (provided the proton exchange is hindered), in contrast to the J_{N2H1} coupling, which seems too small.

The similarity of the nitrogen−hydrogen system in Figure 1 with the cavity of porphyrin and porphycene suggests that 2ABAI constitutes a useful test molecule for the calculation of NMR parameters of porphyrin and porphycene. Therefore, we take the good performance of the B3LYP/Huz-IIsu2 method on 2ABAI as an indication that this level of theory is appropriate for the study of NMR parameters in porphyrin and porphycene.

C. Indirect Nuclear Spin−Spin Coupling Constants of Porphyrin and Porphycene. *1. Spin−Spin Coupling Constants at the Equilibrium Geometries.* In our discussion, we shall concentrate on two of the most interesting types of spin−spin coupling constants in porphyrin and porphycene, that is, the J_{NH} coupling constants between an inner proton and one of the four nitrogen nuclei and the J_{HH} through-space spin−spin coupling constants between the two inner protons. For the global minimum trans structures, these coupling constants are listed in Table 2.

The covalently transmitted spin−spin coupling constants $^1J_{NH}$ have similar values in porphyrin and porphycene: −108.47 and −97.52 Hz, respectively. Like most one-bond nitrogen−proton couplings,[47] they are dominated by the Fermi-contact (FC) term; the diamagnetic spin−orbit (DSO), paramagnetic spin−orbit (PSO), and spin-dipole (SD) terms do not exceed ±1.00 Hz.

In porphyrin, the coupling constants of the hydrogen nucleus H1 with two neighboring nitrogen nuclei (N1 and N3) are equal by symmetry and, like the covalently transmitted coupling $^1J_{N4H1}$, they are dominated by the FC term. The small, negative J_{N2H1} constant is dominated by the spin−orbit interactions. In this respect, it resembles long-range through-space couplings more than hydrogen-bond-transmitted couplings, in agreement with the arrangement of the coupled nuclei in the trans structure of porphyrin. Since the sum of the spin−orbit terms decays much slower with the internuclear distance than does the FC term (i.e., as R^{-3} rather than exponentially), the dominance of the spin−orbit terms at long distances is not surprising.[48] An interesting feature of the nitrogen−proton couplings is the sign changes, which are determined by the FC term: J_{N4H1} is negative, J_{N1H1} is positive, and J_{N2H1} is negative again. We shall return to this point later, when we discuss the changes in the coupling constants upon proton transfer.

In porphycene, the coupling constants of H1 with the two neighboring nitrogen nuclei (N1 and N3) are different. The J_{N1H1} coupling constant is quite large (3.28 Hz), and it is dominated

by the FC term. The much smaller J_{N3H1} coupling is also dominated by the FC term, since the two large spin−orbit terms nearly cancel. As in porphyrin, J_{N2H1} is very small and dominated by the spin−orbit terms, with the FC and SD terms being negligible.

The J_{HH} spin−spin coupling constants between the inner protons are positive, which means that the reduced values of these constants and of the hydrogen-bond-transmitted J_{NH} coupling constants (such as J_{N1H1} discussed above) have opposite signs. In most of the porphyrin and porphycene structures, the FC and SD terms are very small (less than 0.06 Hz) and the main contribution to these proton−proton coupling constants comes from the relatively large spin−orbit terms. In porphyrin, the DSO and PSO contributions are about 6 and −5 Hz, respectively; in porphycene, they are 5 and −4 Hz, respectively. The sum of all four terms gives total J_{HH} spin−spin coupling constants in the range 1.0−1.5 Hz. The relative magnitudes of the contributions to the J_{HH} couplings in porphyrin and porphycene therefore resemble those of the couplings between the protons forming adjacent hydrogen bonds in formamide[6] and formic acid[5] dimers.

2. Variation of the J_{NH} Spin−Spin Coupling Constants with Proton Migration. There are four types of J_{NH} spin−spin coupling constants in each molecule (for numbering, see Figures 2 and 3):

(1) The $J_{NH}^{(a)}$ coupling constants between the migrating proton and the nitrogen atom that the proton migrates away from (e.g., J_{N1H1} for the cis-to-trans pathway).

(2) The $J_{NH}^{(b)}$ coupling constants between the migrating proton and the nitrogen atom that the proton migrates toward (e.g., J_{N4H1} for the cis-to-trans pathway).

(3) The $J_{NH}^{(c)}$ coupling constants between the migrating proton and the nitrogen atom adjacent to the one that the proton migrates away from, in some cases bound to the second inner proton (e.g., J_{N2H1} for the cis-to-trans pathway).

(4) The $J_{NH}^{(d)}$ coupling constants between the migrating proton and the nitrogen atom that is the furthest away from the migrating proton (e.g., J_{N3H1} for the cis-to-trans pathway).

The behavior of the $J_{NH}^{(a)}$ coupling constants is depicted in Figure 5(a)i for porphyrin and in Figure 5(a)ii for porphycene. First, as the migrating proton departs, $J_{NH}^{(a)}$ decreases abruptly in magnitude from about −100 to −40 Hz at the transition states and to zero at 1.55−1.65 Å (faster for porphycene than for porphyrin). At larger distances, $J_{NH}^{(a)}$ becomes positive, goes through a flat maximum, and then decreases again toward zero. The distance dependence is dictated by the FC term, which dramatically dominates the coupling constant.

As expected, the distance dependence of $J_{NH}^{(b)}$ in Figure 5(b)i and ii is the mirror image of the $J_{NH}^{(a)}$ dependence. As the two nuclei approach, $J_{NH}^{(b)}$ increases (in absolute value). It is positive at the initial geometry but decays to zero as the proton is transferred and then changes sign and quickly increases to the large values typical for covalent bonding. Like $J_{NH}^{(a)}$, the $J_{NH}^{(b)}$ coupling is dominated by the FC term.

The changes in the $J_{NH}^{(c)}$ coupling constant (Figure 5(c)i and ii) are small. An exception is the significant increase (up to 1.70 Hz) in the coupling constant for the trans-to-trans′ porphyrin pathway as the proton is transferred, related to the simultaneous migration of two protons (H1 from N4 and H2 from N2) and the final formation of an internal hydrogen bond between H1 and N1. The other irregularity appears for the cis2-to-trans porphycene pathway: $J_{NH}^{(c)}$ first increases slightly, then decreases, changes sign, reaches a minimum at the transition state, and eventually decreases toward zero.

Finally, the $J_{NH}^{(d)}$ coupling constant is small and varies little as the proton is transferred; see Figure 5(d)i and ii. Two significant changes in $J_{NH}^{(d)}$ are observed in porphyrin, for the trans-to-trans′ and cis-to-trans pathways. For the former, near the trans geometry, the coupling between the migrating proton and the nitrogen at the other proton is quite large and a maximum appears for the shortest distance between two inner protons, close to the transition state. The second largest change in $J_{NH}^{(d)}$ is observed for the cis-to-trans porphyrin pathway: the coupling first decreases (i.e., increases in absolute value), reaches a minimum, and, for larger NH distances, monotonically increases to 1.70 Hz as the hydrogen bond is formed. An unexpected effect is observed for $J_{NH}^{(d)}$ in the cis2-to-trans porphycene pathway: it first oscillates close to zero, next increases steeply to 4.23 Hz, and finally decreases to the value characteristic of the trans structure, as the hydrogen bond is formed.

3. Variation of the J_{HH} Spin−Spin Coupling Constants with Proton Migration. The J_{HH} coupling constant in Figure 6 changes little upon proton transfer, in particular, for porphycene (except for the cis2-to-trans pathway as noted below). Indeed, some of the changes are within the range of possible numerical artifacts. While J_{HH} depends nonmonotonically on the NH separation, it decreases monotonically with increasing H···H separation, as is particularly noticeable for the trans-to-trans′ porphyrin pathway. In porphycene, J_{HH} is almost independent of the NH separation except for the cis2-to-trans transfer, where the dependence is much more pronounced: close to the cis2 structure, J_{HH} reaches 4.0 Hz; for larger H···H distances, it decreases to 1.2−1.3 Hz. The reason for this behavior is the short H···H separation of 1.55 Å of the cis2 structure, which enables the separation-sensitive FC term to become large.

Except in the cis2-to-trans transfer, the J_{HH} changes are in all cases determined by the spin−orbit terms, which are much larger than the FC and SD terms. It is interesting to note that, for J_{HH} in porphyrin, the FC term is larger than the SD term; conversely, in porphycene, the SD term outweighs the FC term.

D. NMR Shielding Constants of Porphyrin and Porphycene. *1. NMR Shielding Constants at the Equilibrium Geometries.* Table 2 lists the NMR shielding constants for porphyrin and porphycene at the equilibrium structure. We concentrate here on the shielding constants of the inner nuclei: the four nitrogen nuclei and the inner protons. For the nitrogens, we use the same notation as that in section III.C.2.

For symmetry reasons, the H1 and H2 protons, the N1 and N3 nitrogens, and the N2 and N4 nitrogens are equivalent at the trans structures. However, there is a large difference (in particular, for porphyrin) between the shielding constants of N1 and N3 (not bound to protons) and of N2 and N4 (bound to protons): the former atoms are deshielded, while the latter are shielded. For porphyrin, the calculated intrinsic chemical shift difference between the protonated and deprotonated nitrogen atoms (112 ppm) agrees well with the experimental value (108 ppm) from ref 31. For porphycene, the agreement is poorer: the calculated difference is 83 ppm, while the experimental one is given as 52 or 46 ppm, depending on the transfer mechanism assumed in analysis of the experimental spectra.[28]

The shielding constants for porphycene have been computed in ref 30. For the nitrogen atoms, the values of 13 and 104 ppm yield an intrinsic chemical shift of 91 ppm, which is similar to our result of 83 ppm. There is also a large difference between the shielding anisotropies of the protonated and deprotonated

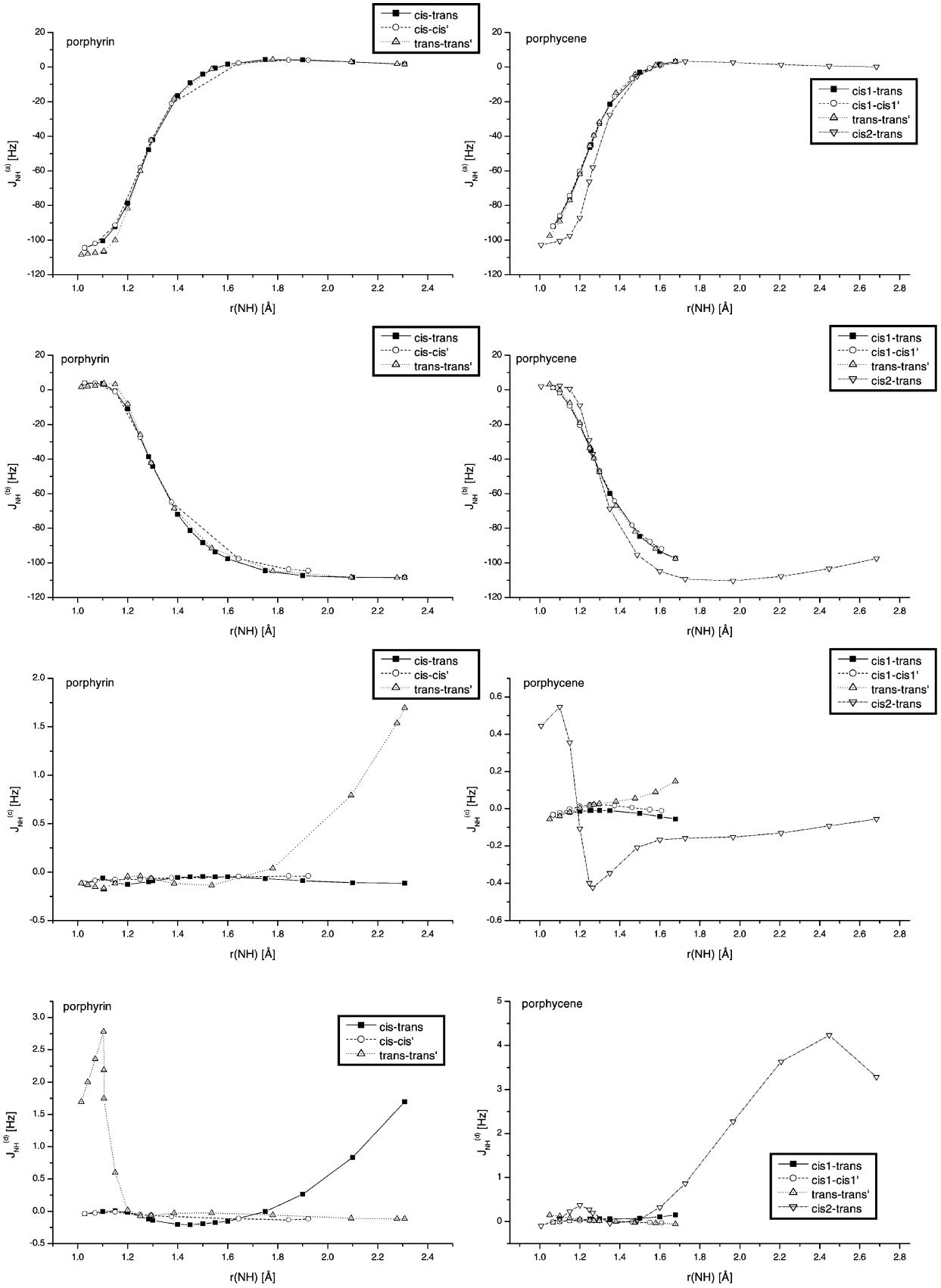

Figure 5. Dependence of J_{NH} coupling constants (in Hz) on the distance between the migrating proton and the parent nitrogen atom (in Å). (a) The spin−spin coupling constants between the migrating proton and the nitrogen atom that the proton migrates away from: (i) porphyrin (left); (ii) porphycene (right). (b) The spin−spin coupling constants between the migrating proton and the nitrogen atom that the proton migrates toward: (i) porphyrin (left); (ii) porphycene (right). (c) The spin−spin coupling constants between the migrating proton and the nitrogen atom adjacent to the one that the proton migrates away from (in some cases bound to the other inner proton): (i) porphyrin (left); (ii) porphycene (right). (d) The spin−spin coupling constants between the migrating proton and the nitrogen atom that is the furthest away from the migrating proton: (i) porphyrin (left); (ii) porphycene (right).

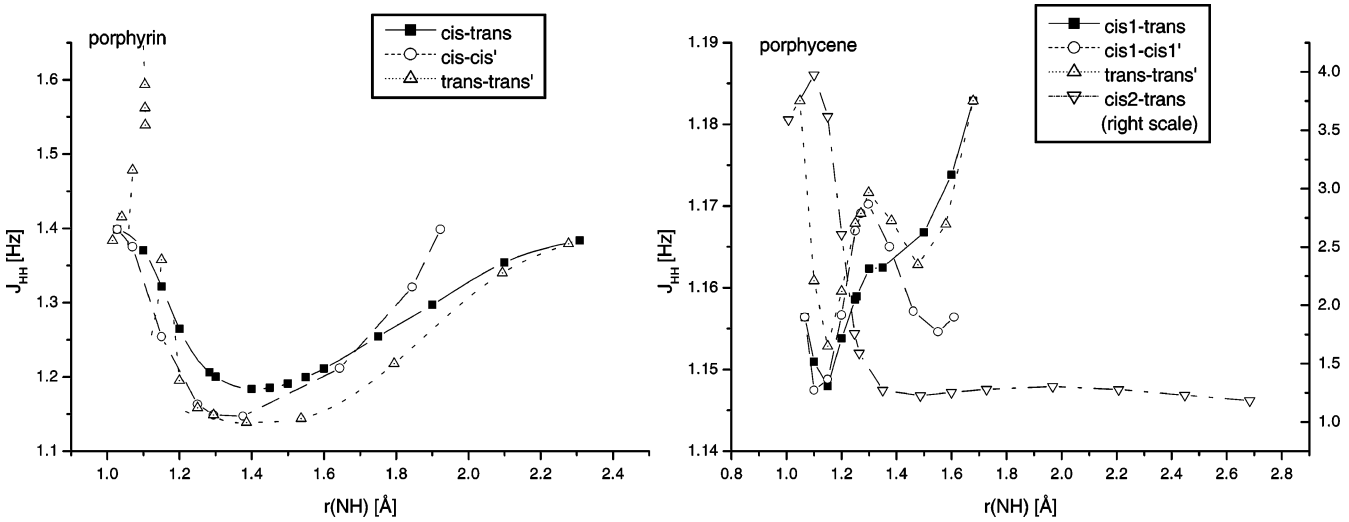

Figure 6. Variation of the J_{HH} coupling constant (in Hz) with the distance between the migrating proton and the parent nitrogen atom (in Å) in porphyrin (left) and in porphycene (right). For the cis2-to-trans pathway in porphycene, the scale is given on the right.

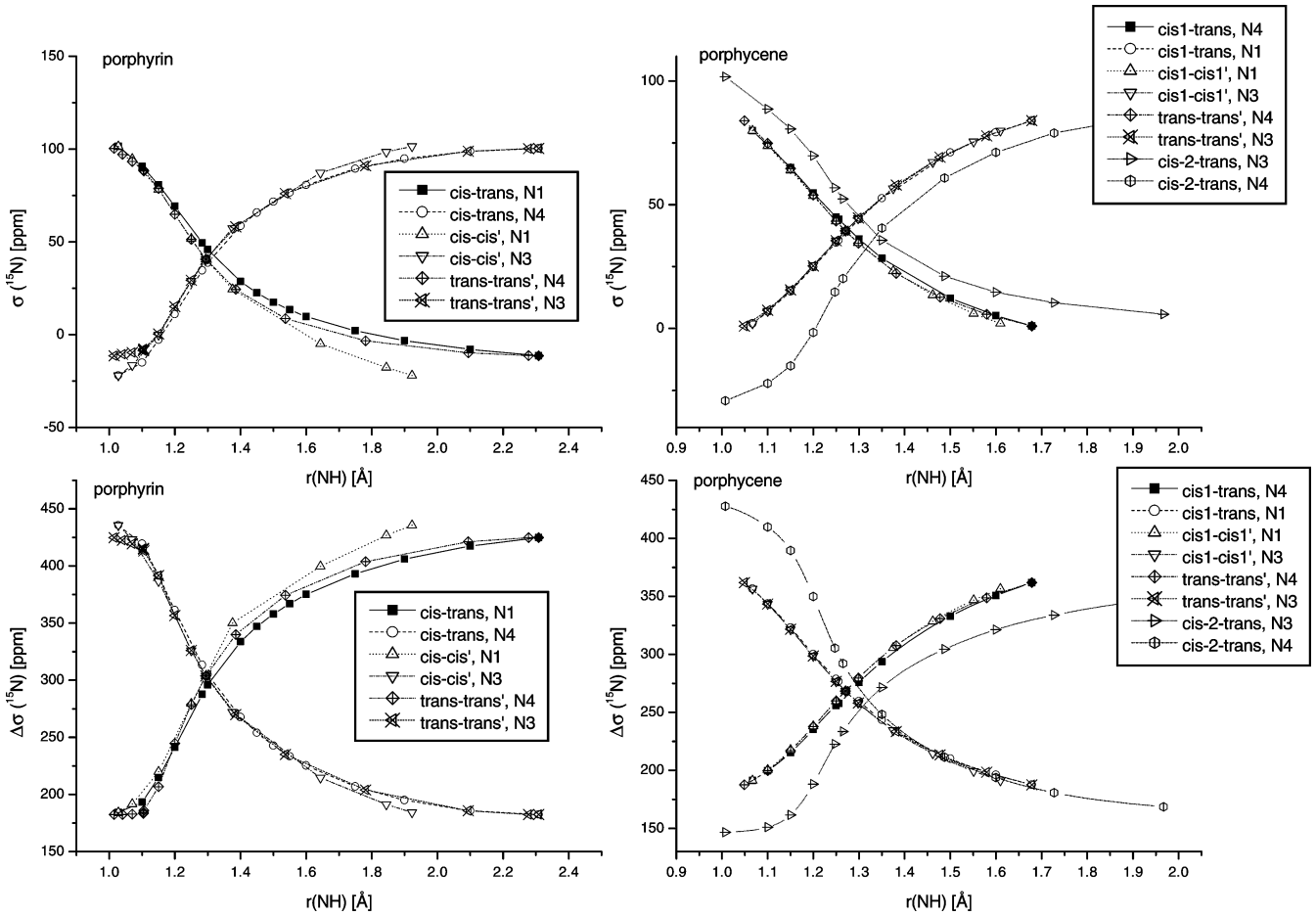

Figure 7. Variation of the isotropic ^{15}N shielding constants (top) and shielding anisotropy (bottom), in ppm, with the distance between the migrating proton and the parent nitrogen atom (in Å) in porphyrin (left) and porphycene (right).

nitrogen atoms. Similar results have been obtained at the GIAO-SCF level in ref 29.

Comparing the inner protons in porphyrin and porphycene, we find that the porphyrin proton is noticeably more shielded in the trans structure. The difference between the calculated shielding constants in the two molecules is in good agreement with experiment, suggesting that again the discrepancies between theory and experiment may be largely due to the conversion of computed shieldings to chemical shifts.

2. Changes in the Nitrogen Shielding Constants upon Proton Migration. The changes in the nitrogen shielding constants plotted in Figure 7 follow the same pattern for all (single and double) exchange mechanisms. They are substantial and monotonic: while the parent nitrogens become deshielded upon migration, the terminal nitrogens become shielded. All changes are in the 80−100 ppm range, depending on the pathway and the molecule. For the single proton transfers cis-to-trans, cis1-to-trans, and cis2-to-trans in porphycene, the shielding constants

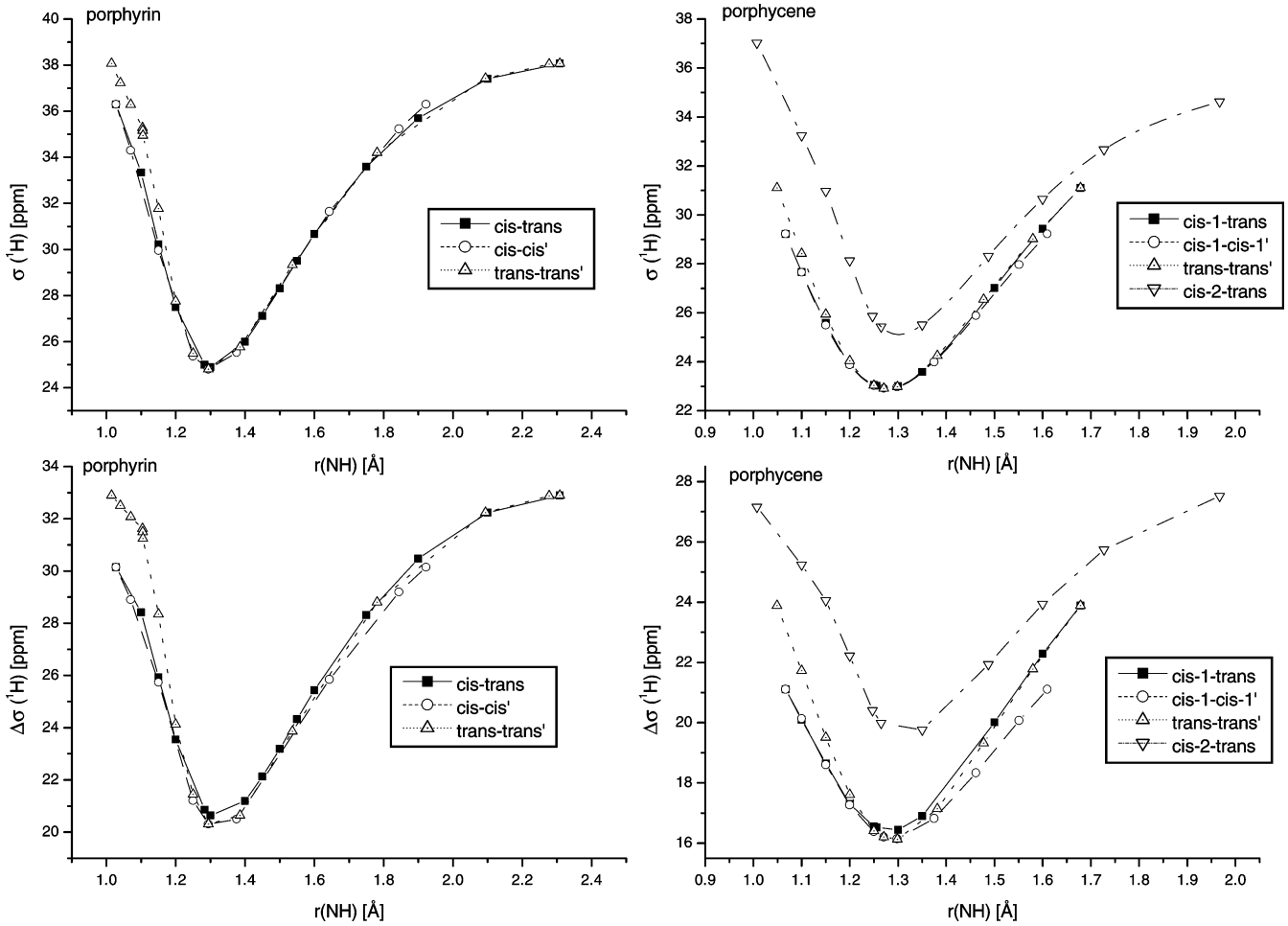

Figure 8. Variation of the isotropic ^{1}H shielding constants (top) and shielding anisotropy (bottom), in ppm, with the distance between the migrating proton and the parent nitrogen atom (in Å) in porphyrin (left) and porphycene (right).

of the two spectator nitrogens (not shown in Figure 7) vary only slightly, smoothly changing their values in the course of the migration.

The changes in the anisotropy shieldings of the nitrogen nuclei between which the proton migrates are similar to those in the isotropic shieldings, keeping in mind that the anisotropic values are twice as large as the isotropic ones. The changes are, however, always opposite in the sense that the anisotropy increases when the isotropic shielding decreases, and vice versa. This difference arises from the different behavior of the perpendicular and in-plane shielding components. Whereas the former becomes more positive when the nitrogen atom loses the proton, the latter become more negative. The changes of the in-plane shielding components are much larger than those of the perpendicular component, and consequently, the isotropic average mirrors their behavior.

3. Changes in the Hydrogen Shielding Constants upon Proton Migration. The changes in the shielding of the migrating proton are essentially the same for both molecules and all the pathways; see Figure 8. Upon migration, the proton first becomes deshielded and then shielded again, with the strongest deshielding occurring at the transition state. The variation of the shielding is substantial, 6−13 ppm, spanning almost the whole range of the ^{1}H NMR shielding scale.

Although the shielding of the stationary proton in the cis-to-trans porphyrin pathway and in the cis1-to-trans and cis2-to-trans porphycene pathways (not shown in Figure 8) varies much less than that of the migrating proton, its changes are not negligible, spanning, for example, 3 ppm for the cis-to-trans porphyrin pathway.

The changes in the anisotropy of the shielding constants of the migrating proton follow the changes in isotropic ^{1}H shieldings. They are of the same order of magnitude and have the same direction for the whole range of the N···H distances under study. This similarity of the variation of the anisotropy of the shielding constants of the migrating proton and the variation of the isotropic shielding originates from the fact that the changes of the component perpendicular to the molecular plane and the parallel components are always in the same direction, and those of the perpendicular component span a wider range.

IV. Summary and Conclusions

The NMR spin−spin and shielding constants were calculated for porphyrin and porphycene, and their changes during single and double internal proton transfers were investigated. Additionally, the NMR parameters were calculated for a smaller molecule with an internal proton between a set of nitrogen atoms: 1,3-bis(arylimino)isoindoline. The good agreement of the shielding and spin−spin coupling constants calculated for this compound, which resembles porphyrin and porphycene in that is has a system of N−H···N internal hydrogen bonds, with experimental values suggests that the predictions obtained with our DFT approach are reliable. The results for porphyrin and porphycene, for which the experimental data set is limited, can be summarized as follows.

With respect to the potential energy surfaces of porphyrin and porphycene, our calculations confirm previous findings. We found two energy minima, corresponding to trans and cis geometries, with the energy differences being 34.3 kJ/mol for porphyrin and 9.3 kJ/mol for porphycene. The third tautomer of porphycene, denoted cis2, is a transition state. We have considered seven proton-exchange pathways: we examined the cis-to-trans, trans-to-trans′, and cis-to-cis′ pathways of both molecules; in addition, we analyzed the cis2-to-trans pathway of porphycene. The barrier is highest for the cis2-to-trans porphycene pathway and lowest for the cis-to-cis′ porphycene pathway.

For each pathway, calculations of the spin−spin and shielding constants were carried out. As expected, the couplings most strongly affected by the transfer are the J_{NH} couplings of the migrating proton with the parent and terminal nitrogen nuclei. As the proton migrates and the distance to the parent nitrogen increases, J_{NH} rapidly goes to zero, then increases to a positive value, and finally goes to zero again. While this coupling is dominated by the FC interaction, the spin−orbit interaction contributes significantly to the couplings to the remaining two spectator nitrogens. These couplings are weak but exhibit relatively large changes upon proton migration. Although the J_{HH} coupling constants change little upon migration, they exhibit a shallow maximum close to the transition state, making them interesting as prospective structural parameters. Like the long-range J_{NH} coupling, J_{HH} is determined by the spin−orbit terms except close to the cis2 structure in porphycene, where the proton−proton distance is sufficiently small for the FC term to prevail.

The shielding constants of the inner protons and the nitrogens engaged in the proton transfer change significantly during the migration, with the parent nitrogens becoming deshielded and the terminal nitrogens shielded. The isotropic changes of 80−100 ppm are accompanied by twice as large (and opposite in direction) changes in the shielding anisotropy.

The changes in the isotropic shielding of the migrating proton are substantial, spanning almost the full ^{1}H shielding scale, and they are accompanied by equally large anisotropy changes. The migrating proton first becomes deshielded as it moves toward the transition state and then becomes shielded again as the terminal nitrogen is approached. In the cis-to-trans, cis1-to-trans, and cis2-to-trans pathways, the shielding constants of the stationary proton are essentially unaffected by migration.

Concerning the possibility of measuring and extracting meaningful structural information from the spin−spin coupling constants, the J_{NH} coupling constants between the migrating proton and the parent or terminal nitrogen nuclei appear to be promising in this respect, provided the system is sufficiently cooled to slow the proton motion and enable the measurement. Because of the higher exchange barriers, this should be easier to achieve for porphyrin than for porphycene. For both molecules, the ^{14}N/^{15}N isotopic substitution at selected sites may facilitate the experimental detection of proton-transfer related changes of spin−spin coupling and shielding constants.

Acknowledgment. H.C. would like to express his gratitude to Prof. Kenneth Ruud for his support and for making the computational resources available. M.J. wishes to acknowledge financial support of the Polish grant KBN 4 T09A 038 23. T.H. acknowledges support from the Norwegian Research Council through a Strategic University Program in Quantum Chemistry (154011/420) and through a grant of computer time from the Supercomputing Program (nn1118k).

References and Notes

(1) Brunner, E.; Sternberg, U. *Prog. Nucl. Magn. Reson. Spectrosc.* **1998**, *32*, 21.
(2) Frey, P. A.; Whitt, S. A.; Tobin, J. B. *Science* **1994**, *264*, 1927.
(3) Goswani, B.; Gaffney, B. L.; Jones, R. A. *J. Am. Chem. Soc.* **1993**, *115*, 3832.
(4) Benedict, H.; Shenderovich, I. G.; Malkina, O. L.; Malkin, V. G.; Denisov, G. S.; Golubev, N. S.; Limbach, H.-H. *J. Am. Chem. Soc.* **2000**, *122*, 1979.
(5) Pecul, M.; Leszczynski, J.; Sadlej, J. *J. Chem. Phys.* **2000**, *112*, 7930.
(6) Pecul, M.; Leszczynski, J.; Sadlej, J. *J. Phys. Chem. A* **2000**, *104*, 8105.
(7) Pecul, M.; Lewandowski, J.; Sadlej, J. *Chem. Phys. Lett.* **2001**, *333*, 139.
(8) Pecul, M.; Sadlej, J.; Leszczynski, J. *J. Chem. Phys.* **2001**, *115*, 5498.
(9) Pecul, M.; Sadlej, J. In *Computational Chemistry: Reviews of Current Trends*; Leszczynski, J., Ed.; World Scientific: Singapore, 2003; Vol. 8, pp 131−160 (Ab initio calculations of the intermolecular nuclear spin−spin coupling constants).
(10) Karger, N.; Amorin da Costa, A. M.; Ribeiro-Claro, P. J. A. *J. Phys. Chem. A* **1999**, *103*, 8672.
(11) Cerioni, G.; Biali, S. E.; Rappoport, Z. *Tetrahedron Lett.* **1996**, *37*, 5797.
(12) Juranic, N.; Ilich, P. K.; Macura, S. *J. Am. Chem. Soc.* **1995**, *117*, 405.
(13) Cordier, F.; Grzesiek, S. *J. Am. Chem. Soc.* **1999**, *121*, 1601.
(14) Cornilescu, G.; Hu, J.-S.; Bax, A. *J. Am. Chem. Soc.* **1999**, *121*, 2949.
(15) Cordier, F.; Rogowski, M.; Grzesiek, S.; Bax, A. *J. Magn. Reson.* **1999**, *140*, 510.
(16) Dingley, A. J.; Grzesiek, S. *J. Am. Chem. Soc.* **1998**, *120*, 8293.
(17) Dingley, A. J.; Masse, J. E.; Peterson, R. D.; Barfield, M.; Feigon, J.; Grzesiek, S. *J. Am. Chem. Soc.* **1999**, *121*, 6019.
(18) Helgaker, T.; Jaszuński, M.; Ruud, K. *Chem. Rev.* **1999**, *99*, 293.
(19) Vaara, J.; Jokisaari, J.; Wasylishen, R. E.; Bryce, D. L. *Prog. Nucl. Magn. Reson. Spectrosc.* **2002**, *41*, 233.
(20) Contreras, R. H.; Barone, V.; Facelli, J. C.; Peralta, J. E. *Ann. Rep. NMR Spectrosc.* **2003**, *51*, 167.
(21) Kaupp, M.; Bühl, M.; Malkin, V. G. *Calculation of NMR and EPR parameters. Theory and applications*; Wiley-VCH: Weinheim, Germany, 2004.
(22) Cleland, W. W.; Frey, P. A.; Gertl, J. A. *J. Biol. Chem.* **1998**, *273*, 25529.
(23) Scheiner, S.; Kar, T. *J. Am. Chem. Soc.* **1995**, *117*, 6970.
(24) Guthrie, J. P.; Kluger, R. *J. Am. Chem. Soc.* **1993**, *115*, 11569.
(25) Waeshel, A.; Papazyan, A.; Kollman, P. A. *Science* **1995**, *269*, 103.
(26) Gertl, J. A.; Gassman, P. G. *J. Am. Chem. Soc.* **1993**, *115*, 11552.
(27) Braun, J.; Schlabach, M.; Wehrle, B.; Köcher, M.; Vogel, E.; Limbach, H.-H. *J. Am. Chem. Soc.* **1994**, *116*, 6593.
(28) Langer, U.; Hoelger, C.; Wehrle, B.; Latanowicz, L.; Vogel, E.; Limbach, H.-H. *J. Phys. Org. Chem.* **2000**, *13*, 23.
(29) Kozlowski, P. M.; Wolinski, K.; Pulay, P.; Ye, B.-H.; Li, X.-Y. *J. Phys. Chem. A* **1999**, *103*, 420.
(30) Steiner, E.; Fowler, P. W. *Org. Biomol. Chem.* **2003**, *1*, 1785.
(31) Wehrle, B.; Limbach, H. H.; Köcher, M.; Ermer, O.; Vogel, E. *Angew. Chem., Int. Ed. Engl.* **1987**, *26*, 934.
(32) Vogel, E.; Köcher, M.; Schmickler, H.; Lex, *J. Angew. Chem., Int. Ed. Engl.* **1986**, *26*, 257.
(33) Schilf, W. *J. Mol. Struct.* **2004**, *691*, 141.
(34) Becke, A. D. *J. Chem. Phys.* **1993**, *98*, 5648.
(35) Frisch, M. J.; Trucks, G. W.; Schlegel, H. B.; Scuseria, G. E.; Robb, M. A.; Cheeseman, J. R.; Zakrzewski, V. G.; Montgomery, J. A.; Stratmann, R. E.; Burant, J. C.; Dapprich, S.; Millam, J. M.; et al. *Gaussian 98*, revision A.1; 1998.
(36) Helgaker, T.; Jensen, H. J. A.; Jørgensen, P.; Olsen, J.; Ruud, K.; Ågren, H.; et al. *DALTON, an ab initio electronic structure program*, release 1.2; 2001 (see http://www.kjemi.uio.no/software/dalton/dalton.html).
(37) Helgaker, T.; Watson, M.; Handy, N. C. *J. Chem. Phys.* **2000**, *113*, 9402.
(38) Helgaker, T.; Wilson, P. J.; Amos, R. D.; Handy, N. C. *J. Chem. Phys.* **2000**, *113*, 2983.
(39) London, F. *J. Phys. Radium* **1937**, *8*, 397.
(40) Huzinaga, S. *Approximate Atomic Functions*, Tech. Rep., University of Alberta, Edmonton, 1971.
(41) Helgaker, T.; Jaszuński, M.; Ruud, K.; Górska, A. *Theor. Chem. Acc.* **1998**, *99*, 175.
(42) Chen, B. M. L.; Tulinsky, A. *J. Am. Chem. Soc.* **1972**, *94*, 4144.
(43) Boronat, M.; Ortí, E.; Viruela, P. M.; Tomás, F. *J. Mol. Struct.* **1997**, *390*, 149.
(44) Kozlowski, P. M.; Zgierski, M. Z.; Baker, J. *J. Chem. Phys.* **1998**, *109*, 5905.
(45) Maity, D. K.; Bell, R. L.; Truong, T. N. *J. Am. Chem. Soc.* **2000**, *122*, 897.
(46) Baker, J.; Kozlowski, P. M.; Jarzecki, A. A.; Pulay, P. *Theor. Chim. Acta* **1997**, *97*, 59.
(47) Pecul, M.; Sadlej, J.; Helgaker, T. *Chem. Phys. Lett.* **2003**, *372*, 476.
(48) Watson, M. A.; Salek, P.; Macak, P.; Jaszuński, M.; Helgaker, T. *Chem.−Eur. J.* **2004**, *10*, 4627.